

On the Electric and Dielectric Properties of Some Boro-Lead Sulphate Glasses

A. A. Atta^a, H. H. Wahba^a, Ali. A. Alkathiri^a, A. L. Waly^b, Bushra Al-hasni^c, and E. M. Ahmed^{d, e, *}

^a Department of Physics, College of Science, Taif University, P.O. box 11099, Taif, 21944 Saudi Arabia

^b Basic Science Department, Higher Institute of Engineering and Technology, New Damietta, Egypt

^c University of Technology and Applied Sciences-Rustaq, Rustaq, Sultanate of Oman

^d Department of Physics, Faculty of Science, Damietta University, New Damietta, 34517 Egypt

^e University of Technology and Applied Sciences-Sohar, Sohar, Sultanate of Oman

*e-mail: eelagwany@du.edu.eg; eelagwany@yahoo.com

Received November 11, 2021; revised January 16, 2022; accepted February 7, 2022

Abstract—Binary oxide glass system of the composition $(100 - x)\text{B}_2\text{O}_3 \cdot x\text{PbSO}_4$ [$0 \leq x \leq 40$] is prepared by the press-quenching technique. The X-ray measurement confirmed the complete amorphous nature of the studied glasses. The values of the bulk density and oxygen ion density shows a continuous increase with increasing of the mol % PbSO_4 , while molar volume values showed some variations as the mol % PbSO_4 increased in the glasses. The electrical conductivities σ_{dc} and σ_{ac} are tested between 303 and 673 kelvin. The dc conductivity, σ_{dc} , is found to follow the Arrhenius equation, with values between 10^{-12} and 10^{-7} S cm^{-1} in the whole temperature range. The activation energies are found between 0.44 and 0.76 eV. The ac conductivity, σ_{ac} , is determined at four frequencies 120, 10^3 , 10^4 and 10^5 Hz. σ_{ac} for the studied glasses are fitted using the percolation path approximation mechanism (PPT) in addition to the correlated barrier hopping (CBH) mechanism. Some important parameters are obtained as a result of the fitting to the experimental data by both the PPT and the CBH models. Finally, the dielectric constant ϵ' and dielectric loss ϵ'' are studied as a function of temperature.

Keywords: lead sulphate glasses, electrical relaxation, CBH model, PPT model, dielectric properties

DOI: 10.1134/S108765962203004X

INTRODUCTION

One of the most common glass formers is the boron oxide; it is usually used in manufacturing the commercially glasses. Some specific features make the B_2O_3 to be a good glass former, these features are: high bond strength, low cation size and small heat of fusion. The construction of glassy B_2O_3 consists of a random matrix of BO_3 triangles connected by B–O–B bonds [1–4]. Introducing different inorganic cations to the glassy B_2O_3 is found to change the boron coordination from 3 to 4 and leads to the formation of various cyclic units like diborate, triborate or tetraborate groups [5–7]. In the case of borate glass doped with low modifier content, the BO_4 units are grouped to form tetraborate units. Increasing the content of modifier in B_2O_3 glasses, the BO_4 units are mostly connected with diborate groups. At high modifier content glasses, the development of BO_3 units with non-bridging atoms is recommended [8]. Moreover, the PbSO_4 doped B_2O_3 glasses possess both Pb^{2+} ions and $[\text{SO}_4]^{2-}$ groups. The $[\text{SO}_4]^{2-}$ groups mainly contribute to the network

replacing the reduced BO_3 and BO_4 groups [2, 9]. The Pb^{2+} ions will thus become bounded in the structural gaps as alkali cations or will act as bridges between the network forming units [10]. Lead borate glasses present important applications like white LEDs, luminescence, laser technology, photonics and optoelectronic devices and sealing applications [11–15].

Several factors are affecting the disorderly in amorphous semiconductors; such factors are like composition fluctuations, thermal history of the samples and potential fluctuations. This potential fluctuation controls the conduction band edge of the materials. It was estimated by many authors that the density of states in oxide glasses deduced from ac conductivity studies are about 10^{19} to 10^{21} cm^{-3} , and these higher values suggests that the conduction via hopping is probably occurs in the band tails [16–21]. Therefore, the potential fluctuation in the studied glasses can be considered via macroscopic models as in microscopic models.

Two points of views are assumed to explain the origin of the ac conduction. One assumes the solid is consists of a random independent potential barriers

Table 1. Detailed structure of the $B_2O_3 \cdot PbSO_4$ glasses, density of oxygen ions (NO-ion), mean spacing between the Pb-ions (RPb-ion), density of states (N), relaxation time (τ_0), maximum barrier height (W_m) and empirical parameter of the Cole–Cole equation

Sample Name	Composition, mol %	$N_{O-ion} \times 10^{22}$, cm^{-3}	$N_{Pb-ion} \times 10^{21}$, cm^{-3}	R_{Pb-ion} , nm	$N \times 10^{21}$, cm^{-3}	$\tau_0 \times 10^{-13}$, s	W_m , eV	α
PbS0	100B ₂ O ₃ ·0PbSO ₄	5.3	0	0	3.5	0.08	1.4	0.24
								0.28
								0.35
								0.43
PbS1	90B ₂ O ₃ ·10PbSO ₄	6.3	0.5	124	5	1	1.5	0.13
								0.23
								0.36
								0.4
PbS2	80B ₂ O ₃ ·20PbSO ₄	8.3	1.5	87.7	7	1	1.55	0.13
								0.20
								0.30
								0.40
PbS3	70B ₂ O ₃ ·30PbSO ₄	9.1	2.6	72.3	7.4	2	1.7	0.2
								0.24
								0.28
								0.36
PbS4	60B ₂ O ₃ ·40PbSO ₄	9.2	3.9	63.5	8	3	1.8	0.45
								0.49
								0.52
								0.55

(macroscopic look). Here the electronic and ionic conduction cannot be distinguished. It is almost possible to scale measurements of the frequency-dependent conductivity at different temperatures into one single “master” curve. The only common feature of the numerous different solids exhibiting this ac universality is their disorder. Percolation path approximation (PPA) [22, 23], effective-medium approximation (EMA) [24] and random free energy barrier model [25] are examples of such approximations. When looking deep inside the solid, this is the second point of view (microscopic look), which discusses the conductivity only on the bases of electronic, polaronic and ionic relaxation in the band gap. Quantum mechanical tunneling (QMT) [26], correlated barrier hopping (CBH) and its related modification [27–29] are examples of these microscopic models.

Rare studies are found to concern with the conductivity of the glasses doped with PbSO₄. In this article, we aimed to study the electric and dielectric properties of some B₂O₃·PbSO₄ glasses on the light of both the macroscopic and microscopic approaches, to get complete information about the electrical conduction in such types of glasses.

EXPERIMENTAL

In the present work we report on the electrical conductivity in a group of glassy samples with the formula: (100 – x)% B₂O₃· x % PbSO₄, where, x limits from 0 to

40 mol %. The samples names and corresponding compositions are listed in Table 1. The mixed batches are melted between 1000 and 1100°C for 90 min. The melts are stirred several times during melting to ensure homogeneity of the samples. The melts are then poured between two pre-cooled stainless steel plates in the open air. To achieve strain free samples, the matured solid samples are directly moved to a pre-heated furnace at 200°C and let to cool slowly overnight. Parts of the annealed glasses are then polished to obtain disk shape samples, and the other parts are grinded to obtain powder samples. Philips X-ray diffractometer type PW3710 outfitted with Cu tube anode of wavelength $K_{\alpha 1} = 1.54060 \text{ \AA}$ and $K_{\alpha 2} = 1.54439 \text{ \AA}$ is used to examine the structure of the glasses. The generator tension is 40 kV and the generator current is 30 mA. XRD data is collected at angle (2θ) between 10° and 60°. Using the toluene ($\rho_t = 867 \text{ kg/m}^3$) as an emersion liquid, the density of the samples is tested according to Archimedes technique. The electrodes are obtained by painting the opposite flat faces of the disk shape samples by an air drying silver paste to achieve good contacts. The I – V characteristics are carried out to check the ohmic behavior. The measurements of dc conductivity are carried out using 617 Keithly electrometer, whereas ac measurements are done using a computer controlled Stanford LCR bridge model SR 720 at four fixed frequencies 120, 10³, 10⁴ and 10⁵ Hz. All the measurements are carried out in the temperature range from 303 to 673 K.

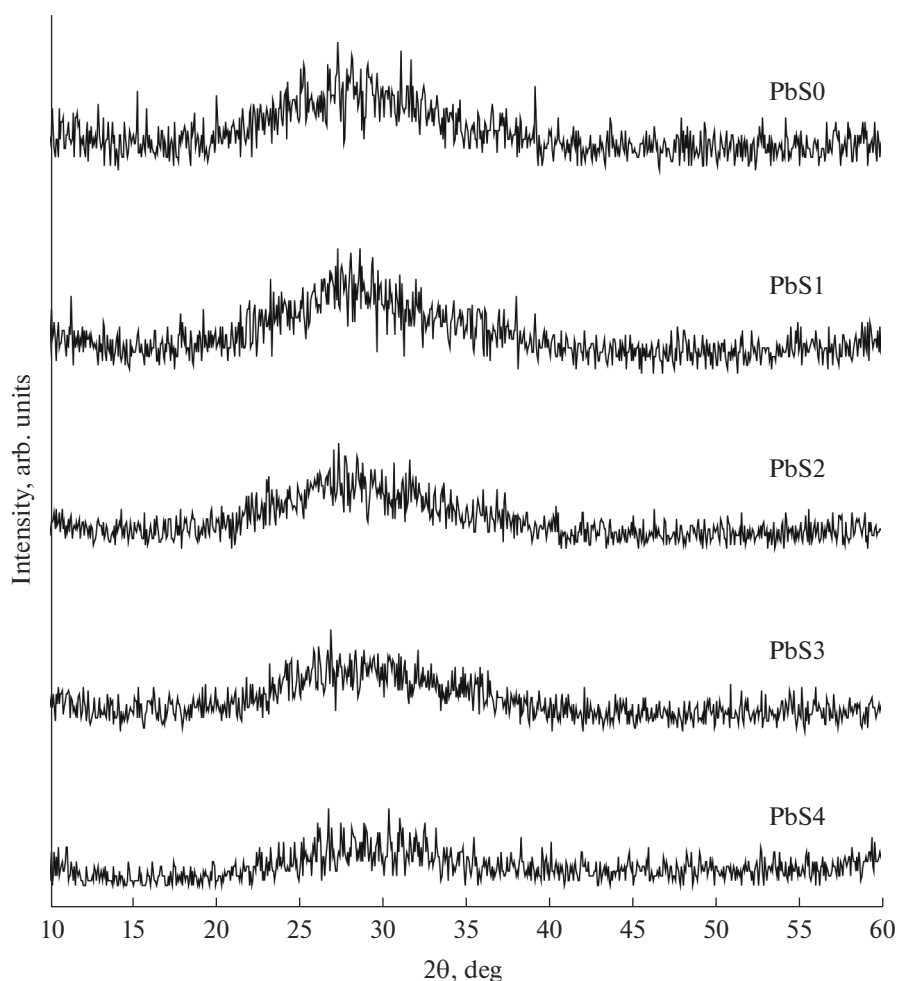


Fig. 1. XRD patterns for the $(100 - x)\text{B}_2\text{O}_3 \cdot x\text{PbSO}_4$ glasses.

RESULTS AND DISCUSSION

X-Ray Diffraction

XRD patterns of the $(100 - x)\% \text{B}_2\text{O}_3 \cdot (x)\% \text{PbSO}_4$ glasses are presented in Fig. 1. From Fig. 1, it is shown that the XRD patterns are detected in the 2θ range from 10° to 60° , with broad humps are shown in all samples round $2\theta \approx 28^\circ$. The presented XRD graphs approve the general amorphous nature and provide a conventional degree of the homogeneity of all the studied glasses. Also, it is noted that there is slightly continuous decreasing of the intensity of the humps on the XRD spectra with increasing of the mol % of PbSO_4 . This decrease of the intensity of the humps may come from the shielding property of the Pb ions and their rule of stopping the X-rays [6].

Density (ρ) and Molar Volume (V_m)

Figure 2 presents the density (ρ) values as a function of lead sulfate content. It is shown that the ρ values increases from 2.05 to 4.92 g/cm^3 with increasing

the PbSO_4 in the glasses. These increases in ρ values can be attributed to the contentious exchanging of the two B atoms (10.81 g/mol) by the heavier Pb atom (207.2 g/mol) and sulfur atom (32.06 g/mol). This is also leads to the gradual formation of somehow compact structure with increasing the PbSO_4 content on the expense of the mol % B_2O_3 in the glasses.

On the other hand, the calculated molar volume (V_m) values are depicted also in Fig. 2 as a function of mol % PbSO_4 . The value of V_m is found to increase from 34 to 35.36 cm^3/mol as the PbSO_4 is just introduced to the matrix. It is suggested that the introduced Pb^{2+} ions and/or $[\text{SO}_4]^{2-}$ groups act to contribute to the glass network, which in turn may increase or widen the vacancies inside glass matrix [2, 3, 9]. More addition of the mol % PbSO_4 up to 20% is found to decrease the values of the V_m . This is may be due to the more additions of the Pb ions tend to fill the empty spaces within the glass network, and hence slightly close the glass matrix. The more increase of the mol % PbSO_4 in the glass matrix beyond 20% is found to

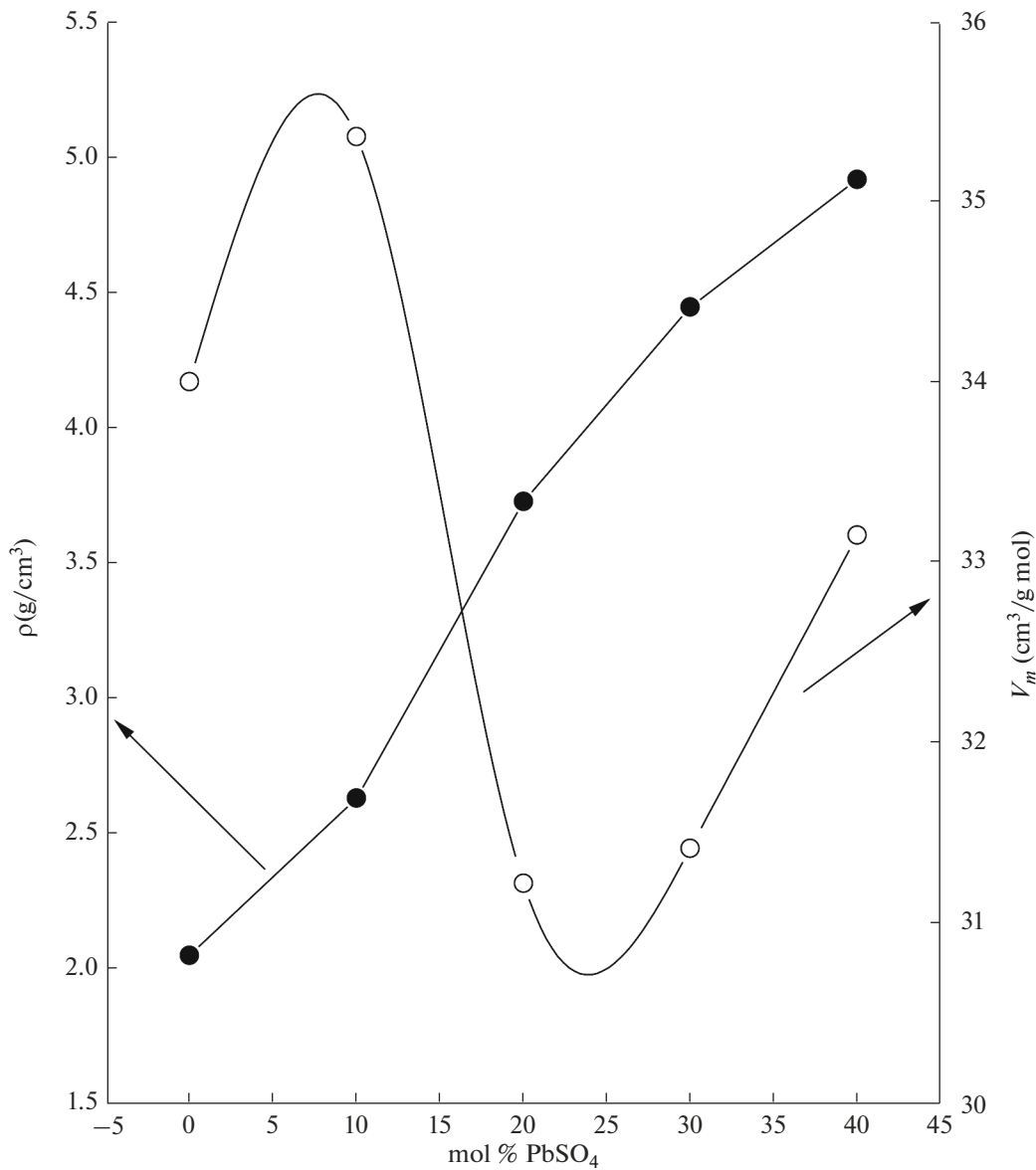


Fig. 2. Density and molar volume values as a function of the mol % of PbSO₄.

increase the V_m values again. At higher lead sulfate content glasses, the increase of the ratio (sulfur oxide/boron oxide) assists the formation of some non-bridging oxygen, which acted in turn to increase the volume occupied by a sample [30].

The O-ion density (N_{O-ion}) can also be computed using the following formula [31]:

$$N_{O-ion} = \rho N_A \left[3 \left(\frac{W_{B_2O_3}}{M_{W(B_2O_3)}} \right) + 4 \left(\frac{W_{PbSO_4}}{M_{W(PbSO_4)}} \right) \right], \quad (1)$$

where W is the weight fraction, M_W is the molar weight of each oxide in a given sample and N_A is the Avogadro's number. The N_{O-ion} values are represented in Table 1. The N_{O-ion} values are found to increase from

5.3×10^{22} to $9.2 \times 10^{22} \text{ cm}^{-3}$ with the increase of mol % PbSO₄. The observed gradually increase of the N_{O-ion} may be due to the gradual increase of the oxygen ions, where every three O-ions from B₂O₃ are substituted by four O-ions from the PbSO₄. As a conclusion, the observed continuous increase of the N_{O-ion} values lead to understand that, as the mol % PbSO₄ increases; the glass network is more unlocked. On the other hand, the Pb-ion density ($N_{Pb-ions}$), can be calculated using the following equation [32]:

$$N_{Pb-ions} = \left[(\rho W_{PbSO_4} / M_{W(PbSO_4)}) N_A \right], \quad (2)$$

where W_{PbSO_4} is the weight ratio of PbSO₄. The $N_{Pb-ions}$ in the glass matrix is found to increase from 5.2×10^{20}

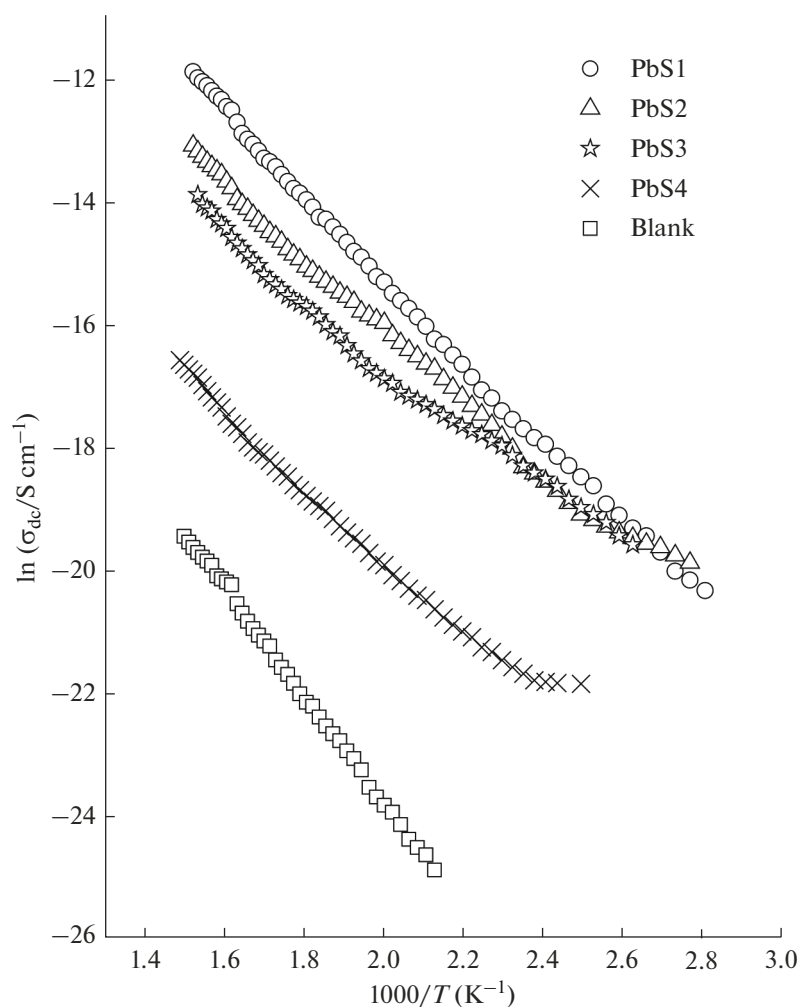


Fig. 3. The dc conductivity as a function of temperature.

to $3.9 \times 10^{21} \text{ cm}^{-3}$ (see Table 1). This may indicate that there is a gradual change in the glass structure due to a gradual increase of the PbSO_4 . In addition, the mean spaces between the *Pb-ions* (R) is computed by Eq. (3) [32] and tabulated in Table 1:

$$R = \left(\frac{1}{N_{\text{Pb-ions}}} \right)^{1/3}. \quad (3)$$

From Table 1, R is found to continue decrease from 124 to 63 nm for the PbSO_4 containing samples. This may suggest that, the jumping electrons/polarons become able to move easily between different oxidation states offered by *Pb-ions* and *B-ions*. These results may conclude that: as the PbSO_4 is gradually increased in the samples, the glass network becomes more closed due to the following reasons: the gradual increase of the O-ions with increasing the PbSO_4 content on the expense of B_2O_3 , the excessive tendency of formation of S^{2-} ions and $[\text{SO}_4]^{2-}$ groups during the cooling of glass melts [2, 9], where $[\text{SO}_4]^{2-}$ groups

should be the major species in the oxidized melts and hence governor the sulfur mobility. Besides, the stronger the oxidizing circumstances throughout the glass melt stage the lower the concentration of S^{2-} cations to be expected, which determines the sulfur transport in the matrix. This means that the sulfur ions have very limited function in the conduction mechanisms, the housing of the Pb^{2+} ions (ionic radii = 119 pm) mainly in the gap positions inside the glass network. Furthermore, the Pb-ions is strongly suggested to share in the Pb rich samples in the glass network as a glass former and halt some of the B–O–B linkages and form some non-bridging oxygens [3, 9].

For these reasons, $[\text{SO}_4]^{2-}$ groups are supposed to substitute the glass forming BO_3 groups to introduce in the glass matrix as a former. Accordingly, this makes the jumping electrons/polarons become able to move easily between Pb and B ions.

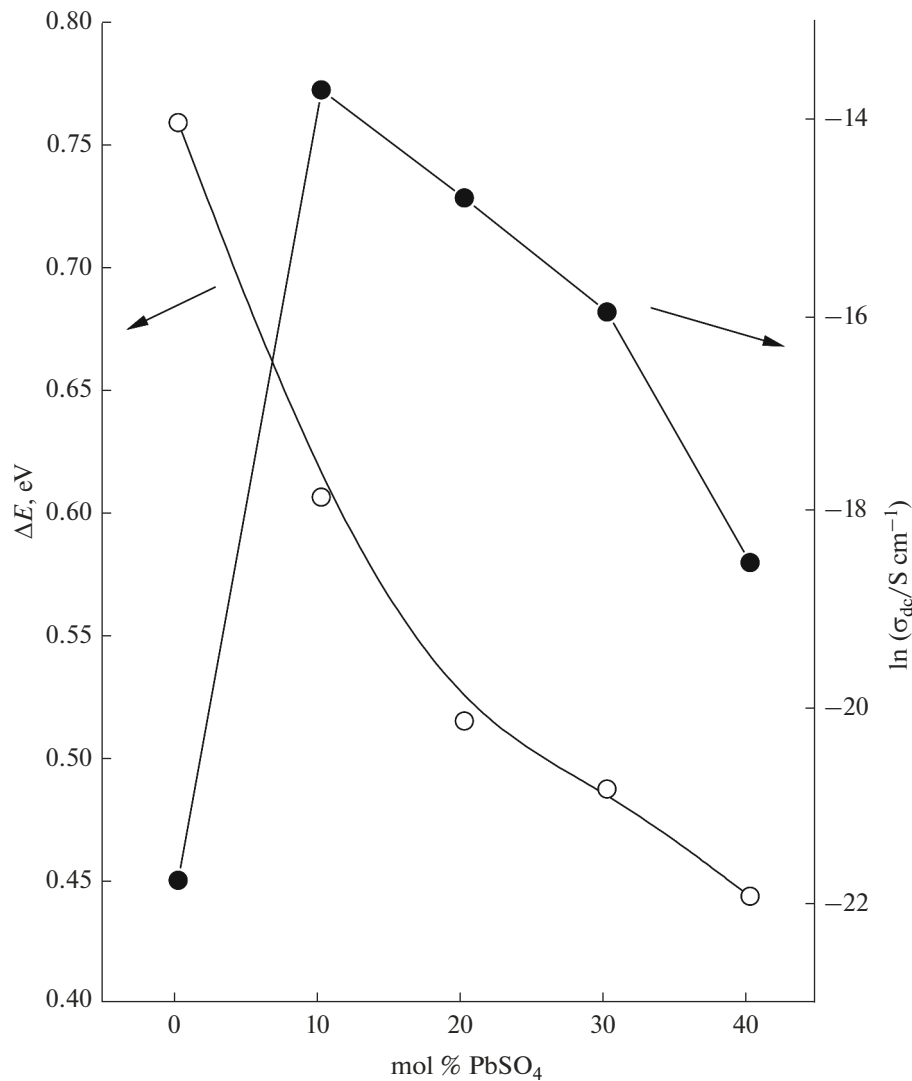


Fig. 4. The dc activation energy and conductivity as a function of the mol % PbSO₄.

dc Conductivity, σ_{dc}

Figure 3 addresses the temperature dependent dc conductivity, σ_{dc} , for all of the examined glasses. In general, the σ_{dc} values are discovered to increase from $1.5 \times 10^{-11} \Omega^{-1} \text{cm}^{-1}$ to $8.2 \times 10^{-6} \Omega^{-1} \text{cm}^{-1}$ with increasing the temperature. The obtained data show a straight line relation for all of the measured samples. These straight lines recommend that the conductivity is a result of thermally activated transition, which can be depicted by the ordinary Arrhenius relation [33–35]:

$$\sigma_{dc} = \sigma_o \exp\left(-\frac{\Delta E}{kT}\right), \quad (4)$$

where σ_o is a constant, ΔE is the activation energy and k is the Boltzmann constant. A feeble deviation from linearity is distinguished in the low temperature area for the glasses with larger than 20 mol % PbSO₄. ΔE are determined and introduced in Fig. 4 as a function

of the mol % PbSO₄. The most extreme activation energy is found to belongs to the PbSO glass and reduce constantly with growing the mol % PbSO₄. Additionally, the compositional reliance of σ_{dc} is shown in Fig. 4. The lowest value of the σ_{dc} is found to exhibit the PbSO glass. As the lead sulfate introduced to the glass matrix, σ_{dc} value is found to increase to the maximum. The further increment of the lead sulfate in the glass is found to decrease the σ_{dc} values in these glasses continuously. The compositional reliance of the ΔE and σ_{dc} magnitudes can be discussed as follows:

In the PbSO sample, the noticed high ΔE and low σ_{dc} magnitudes may come from the way that incredibly all the boron molecules are restricted to form the glass network. Thus, the valence electrons require enormous ΔE to break the bonds and move to the conduction state. As the PbSO₄ is added to the glass; σ_{dc} increased strongly to its most elevated worth and ΔE is

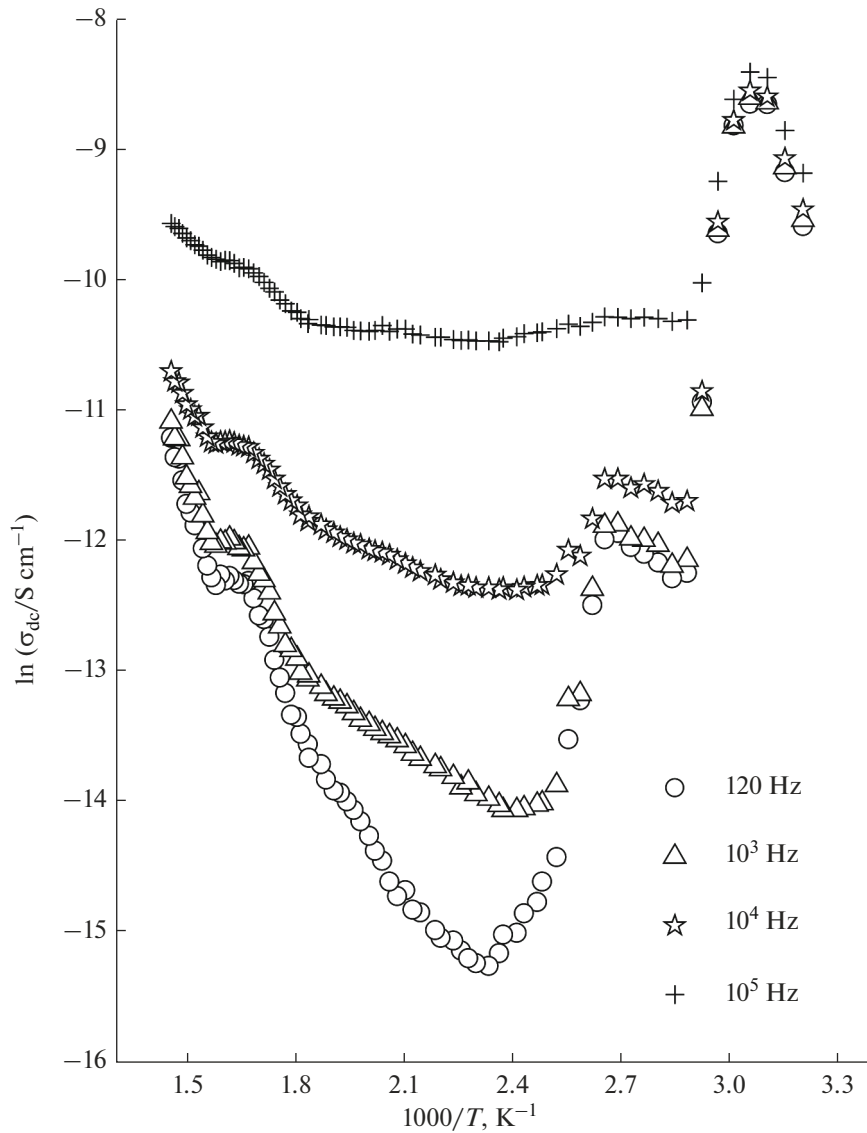


Fig. 5. The ac conductivity as a function of the temperature.

decreased. This might be a direct result of the role of $[\text{SO}_4]^{2-}$ groups, S^{2-} ions and Pb^{+2} which are discussed in detail previously. Furthermore, the continuous increase of the mol % PbSO_4 more than 10% on the expense of the mol % B_2O_3 is found to decrease the molar volume of the glass, which means that the vacancies in the glass are become closer. This may reduce the hopping distance, as well as reduce the number of hopping electrons, which in turn reduces the values for both ΔE and σ_{dc} .

The deviation from linearity that is detected in the samples with more than 20 mol % PbSO_4 in the low temperature region, suggests the weak contribution of another conduction mechanism (ionic or polaronic) beside the dominant electronic mechanism. The new mechanism may come from the possibility of the for-

mation of some S^{2-} anions in the network vacancies, as well as the development of bonds such as Pb-S in the glass matrix [36]. This mixed mechanism may be an additional cause for the continuous decreasing in both the σ_{dc} and the ΔE with the continuous increase of the mol % PbSO_4 in the samples.

ac Conductivity, σ_{ac}

The measured ac conductivity, σ_{ac} , at four fixed frequencies has been plotted against the temperature in Fig. 5 for the PbSO sample. In the low temperature region, σ_{ac} is found almost independent of temperature but large frequency dependence. High temperatures rapidly increase the σ_{ac} , and push it towards the higher frequency with negligible frequency dependence. Similar behavior is qualitatively obtained for all

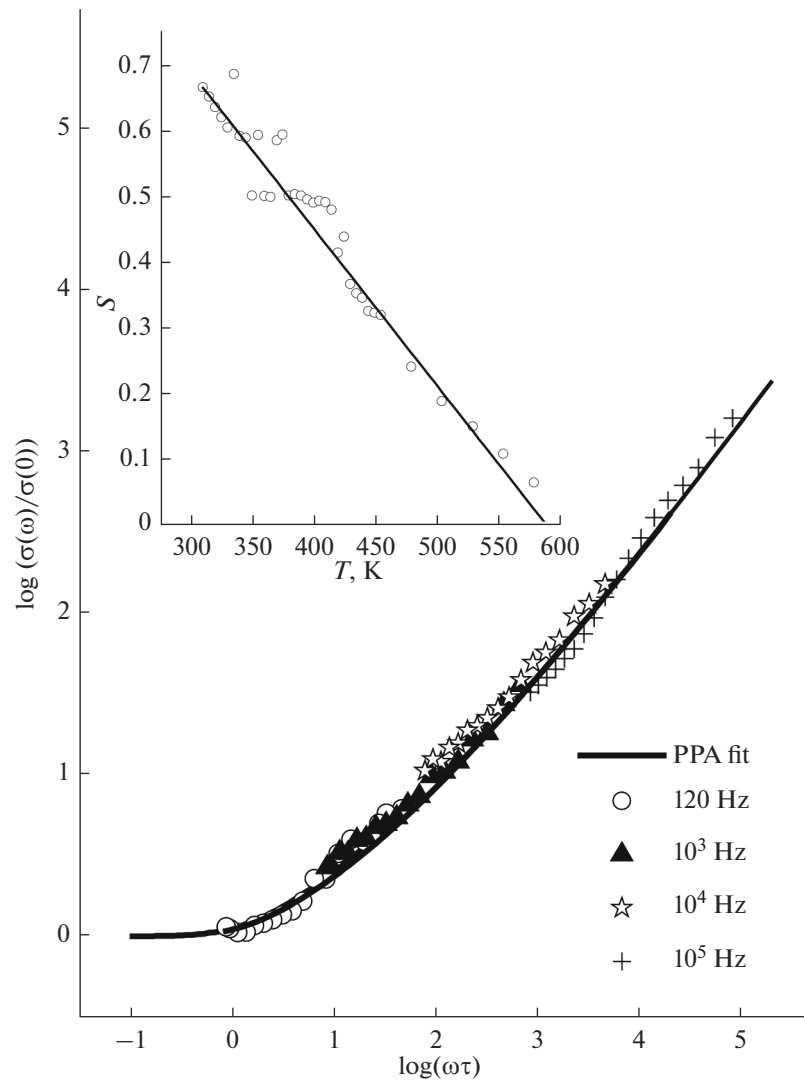


Fig. 6. PPT fitting to the conductivity and its corresponding exponent factor (s).

other glasses. The values of the exponent s are determined from the experimental data applying the equation $s = d \ln(\sigma_{ac})/d \ln(\omega)$ for all the investigated samples.

A significant documentation is noticed for all of the samples except the samples that contain 30 and 40 mol % PbSO_4 . A distortion in the curves is seen lower than 400 K, see Fig. 5. It is seen additionally that this deformation reduces with growing the mol % PbSO_4 content in the glasses. Whereas the B_2O_3 glasses are famous hydrous materials [37–40], the conductivity deformation in the boron rich glasses should arise from the anode polarization impact [41] and the vibration of the OH and water groups [42]. As the temperature increases over 400 K, a traditional σ_{ac} curves is obtained.

Application of percolation path approximation (PPA) model. The percolation path approximation

(PPA) model is planned to be the first mechanism to examine the experimental data. According to this model [43], the hopping of the charge carriers is thermally activated and does not confined to pair of localized sites, and the activation energies are varies randomly. Supposing $P(E)$ to be the local activation energy probability distribution, then the dc activation energy is the highest value. The dc and ac currents are supposed according to the PPA to move in the easiest paths between the electrodes. The conductivity is given by [44]:

$$\frac{\sigma_{ac}}{\sigma_{dc}} = \frac{\omega\tau \arctan(\omega\tau)}{\left[\ln \sqrt{1 + (\omega\tau)^2} \right]^2 + [\arctan(\omega\tau)]^2}, \quad (5)$$

where, τ is the relaxation time:

$$\tau = \frac{\epsilon_{\infty}}{\sigma_{dc}}, \quad (6)$$

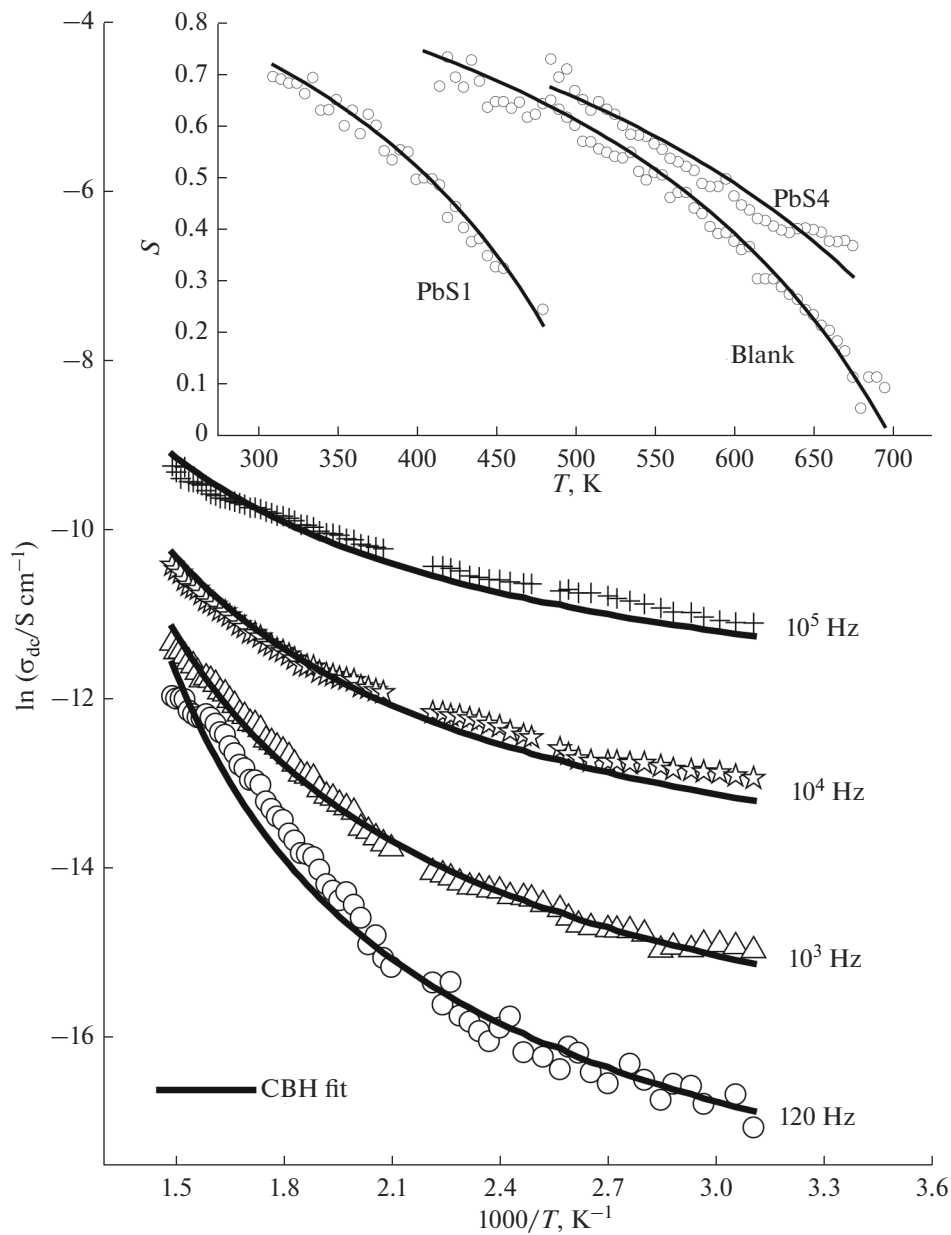


Fig. 7. CBH fitting to the conductivity and its corresponding exponent factor (*s*).

and, σ_{dc} is given by:

$$\sigma_{dc} = \sigma_0 \exp\left(-\frac{E_c}{kT}\right), \quad (7)$$

E_c is the percolation activation energy and is given by:

$$\int_{-E_c}^{+E_c} P(E) dE = P_c, \quad (8)$$

where (P_c) is the percolation threshold [about 0.249 in the 3D].

Figure 6 represents the relation between $\log(\sigma_{ac}/\sigma_{dc})$ and $\log(\omega\tau)$ for the sample PbS2 (data

points), as an example. The solid curves represent the theoretical fitting according to Eq. (5). Good agreement between both the experimental data and the theoretical calculations are obtained for all the samples. The inset in Fig. 6 shows the variation of s with T , and the mathematical fitting of s with T predicted from the following relation [7]:

$$s = \beta - \frac{T}{T_0}, \quad (9)$$

where β is a parameter has value between 1 and 2, also T_0 is a parameter when multiplied with Boltzmann constant k_B gives an energetic look parameter, its value is considered as a measure of the disorderly level in a

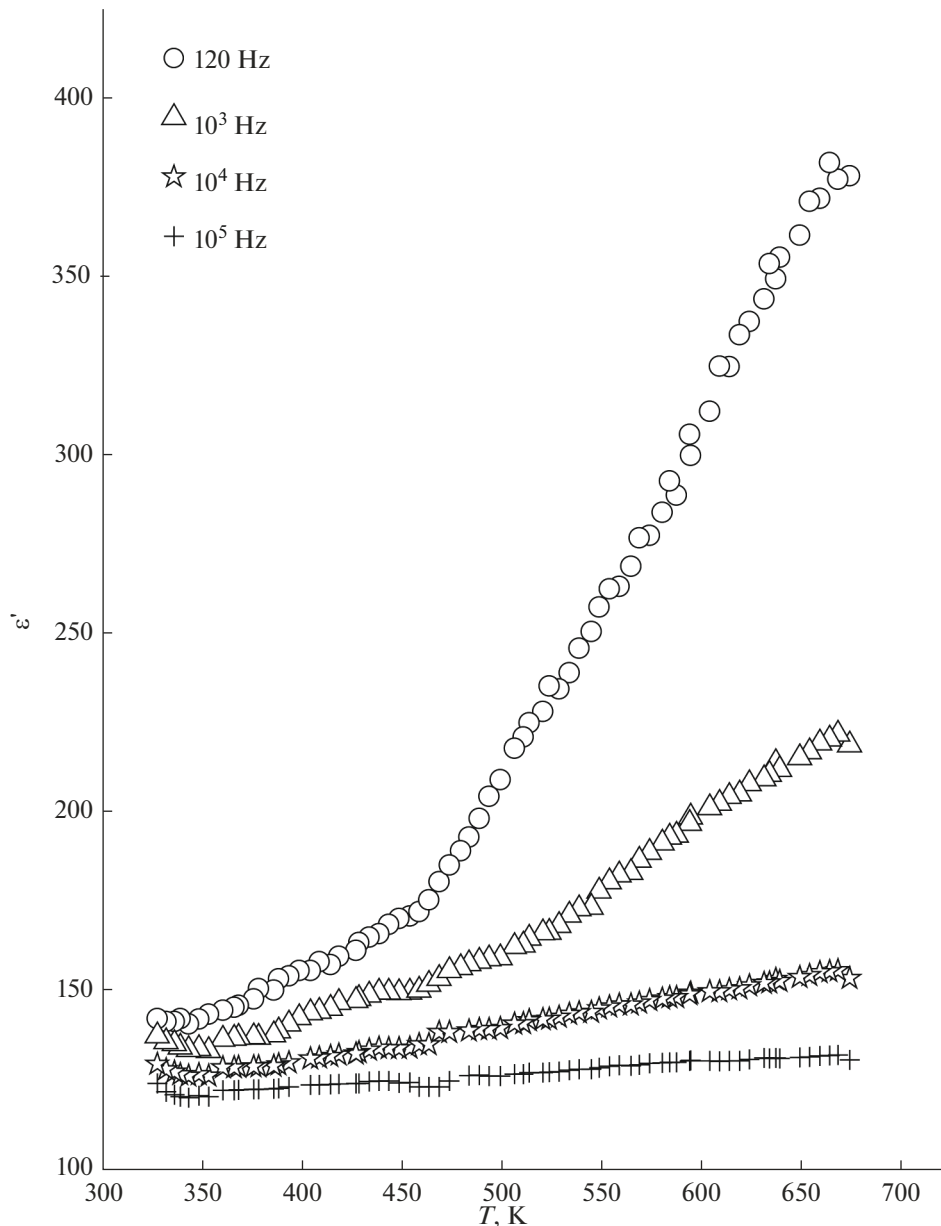


Fig. 8. Temperature dependence of the dielectric constant.

solid. For the present system, β is found to be ≈ 1.4 – 1.8 for all the glasses and $(k_B T_0)$ is found to be between 34.3 and 42.3 meV for all the glasses. In case of $B_2O_3 \cdot Pb_3O_4 \cdot Fe_2O_3 \cdot Na_2O$ glasses [7], $\beta = 2$ and $(k_B T_0) = 26$ – 43 meV; while in case of a-H:Si [1], $\beta = 1$ and $(k_B T_0) = 37.1$ meV.

Application of Correlated Barrier Hopping (CBH) model. The other mechanism suggested to examine the investigational data, is the CBH model. As indicated by this model, the conduction happens through hopping of bipolaron (for example two electrons or polarons jump between charged imperfections D^+ and D^-) over an excited defect states between the different localized states of the present TM-ions. The value of

σ_{ac} according the CBH in the forbidden band gap is given by the equation [27]:

$$\sigma_{ac} = \frac{\pi^3}{24} N^2 \epsilon \epsilon_0 \omega R_\omega^6, \quad (10)$$

where, N is the concentration of pair sites, ϵ is the dielectric constant, ϵ_0 is the permittivity of free space and R_ω is the jumping distance at frequency ω ,

$$R_\omega = \frac{e^2}{\pi \epsilon \epsilon_0 [W_m - kT (1/\omega \tau_0)]}, \quad (11)$$

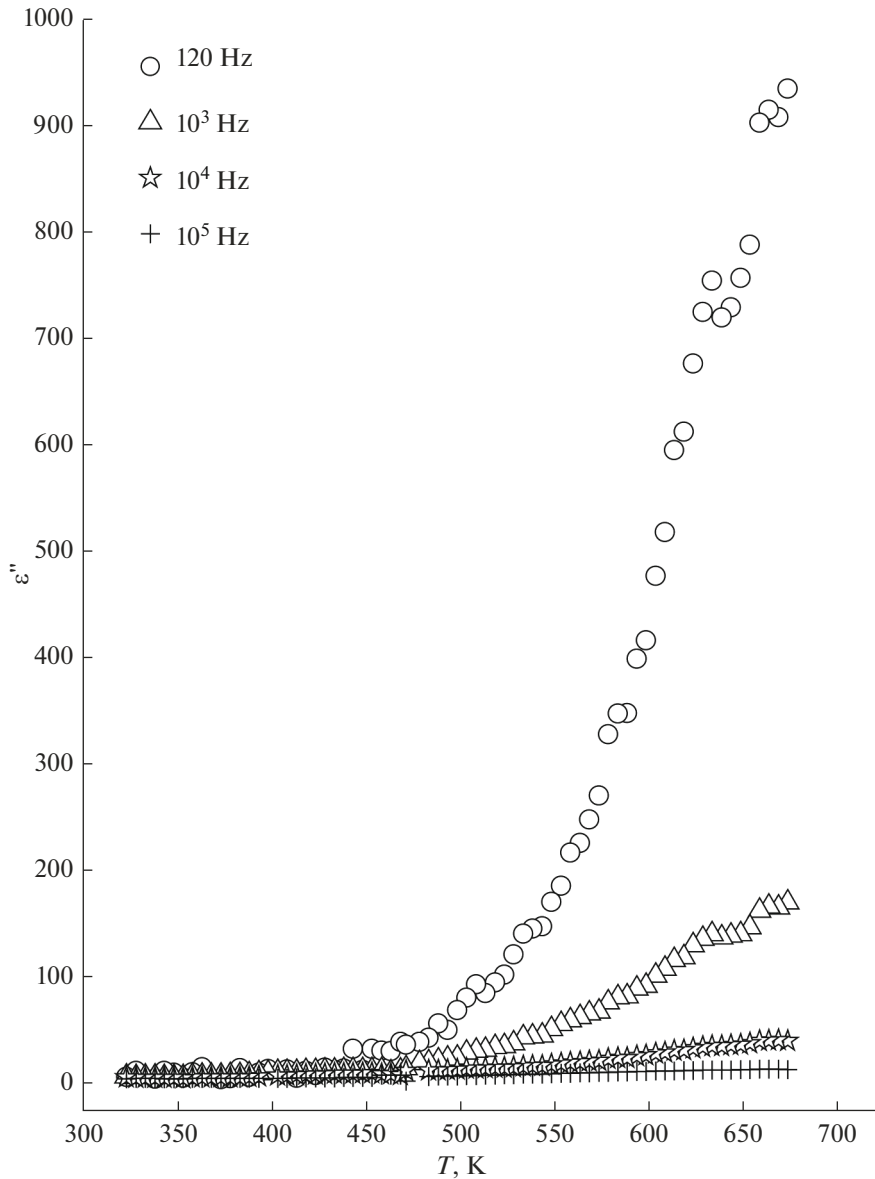


Fig. 9. Temperature dependence of the dielectric loss.

where, e is the electron charge, τ_0 is a constant characteristic relaxation time and W_m is the maximum barrier height.

Finally, the frequency exponent s is computed by using the formula [45]:

$$s = 1 - \frac{6kT}{W_m - [kT \ln(1/\omega\tau_0)]} \quad (12)$$

The fitting of σ_{ac} and s using equations (10)–(12) present a good agreement for the experimental data. The fittings curves are involved in Fig. 7, for the sample PbS4 as an example. From Fig. 7, the CBH fitting of the σ_{ac} seems to be equitable over the whole temperature range. A comparable fitting is attained for all other glasses, representing that the CBH model can also

define the conduction mechanism. A reasonable fitting to the exponent s is displayed inside in Fig. 7 for samples PbS0, PbS1 and PbS4 as examples. This fitting approves the applicability of the CBH model for the examined glasses. N , τ_0 , W_m are some significant parameters gotten from the CBH calculations; they are arranged in Table 1. All the calculated values for N , τ_0 and W_m are established to rise with rising of the mol % PbSO₄ in the glasses.

Dielectric Properties

Figures 8 and 9 show the dielectric constant, $\epsilon'(\omega)$, and the dielectric loss, $\epsilon''(\omega)$, individually, for the glass PbS3 as a function of the temperature. Weak fre-

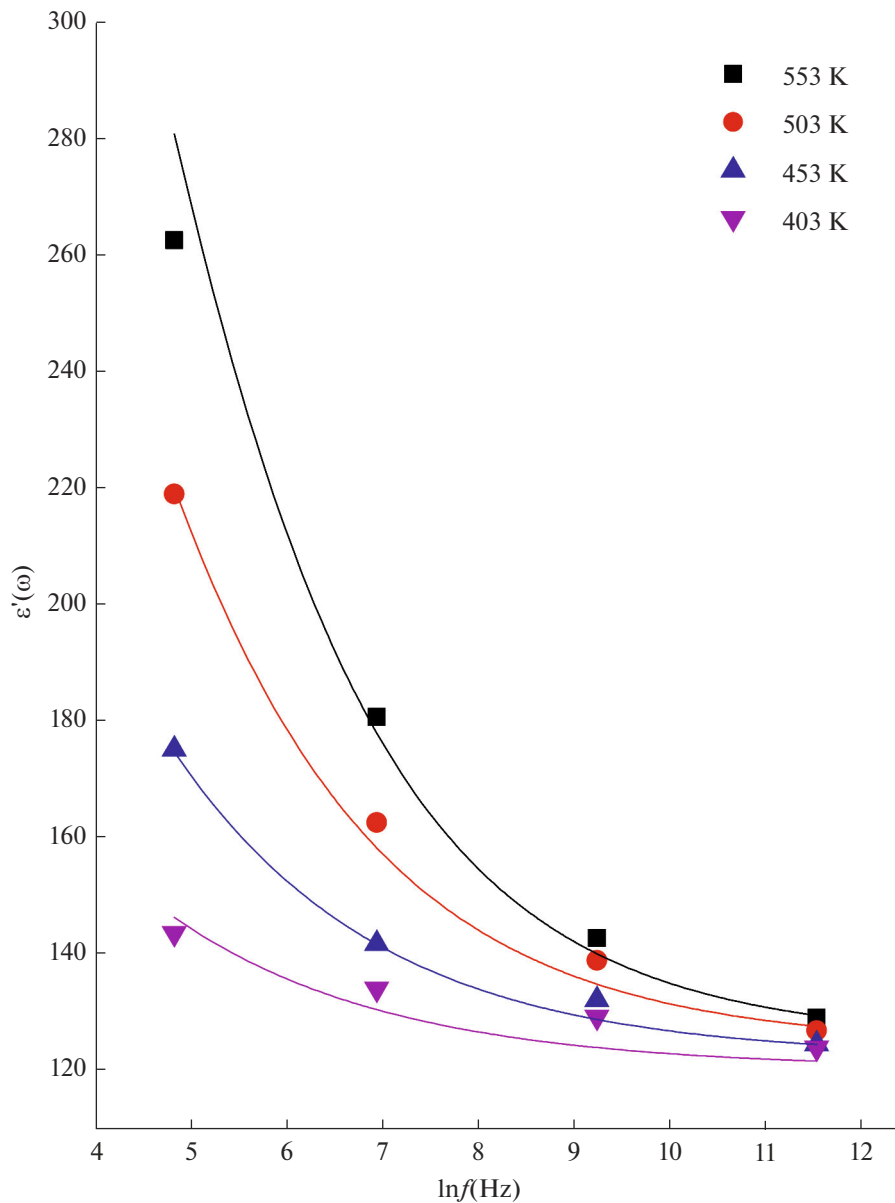


Fig. 10. Frequency dependence of the dielectric constant, solid curves represents the fitting according to Cole–Cole equation.

quency dependence and very nearly temperature independent are seen in the $\epsilon'(\omega)$ and $\epsilon''(\omega)$ curves below 400 K for the dielectric constant and 450 K for the dielectric loss. Over 400 K, a remarkable temperature and frequency dependence are noticed for both $\epsilon'(\omega)$ and $\epsilon''(\omega)$. Comparable values with subjectively slight contrasts are recorded for all of the other glasses. $\epsilon'(\omega)$ noticed for the studied glass samples is generally higher than those noticed for some other regular glasses [46, 47]. It is important to state that, at low frequencies and high temperatures, electrode polarization may have critical effect to the $\epsilon'(\omega)$. Nonetheless, $\epsilon'(\omega)$ is established to be independent of the thickness of the samples and the electrode area at all frequency and temperature ranges. This demonstrates that the

mass impact and the electrode polarization have little effects to the dielectric properties. This shows clearly the impact of the polarizability of lead particles on the dielectric properties of the considered glass samples.

To get more information about the considered glasses, real and imaginary dielectrics for the PbS5 sample are presented in Figs. 10 and 11, individually, as data points. The solid curves signify the attained fitting relating the Cole–Cole equations [48]:

$$\epsilon'(\omega) = \epsilon_{\infty} + \frac{(\epsilon_0 - \epsilon_{\infty}) + (\omega\tau_d)^{(1-\alpha)}(\epsilon_0 - \epsilon_{\infty})\sin(\alpha\pi/2)}{1 + 2(\omega\tau_d)^{(1-\alpha)}\sin(\alpha\pi/2) + (\alpha\tau)^{2(1-\alpha)}}, \quad (13)$$

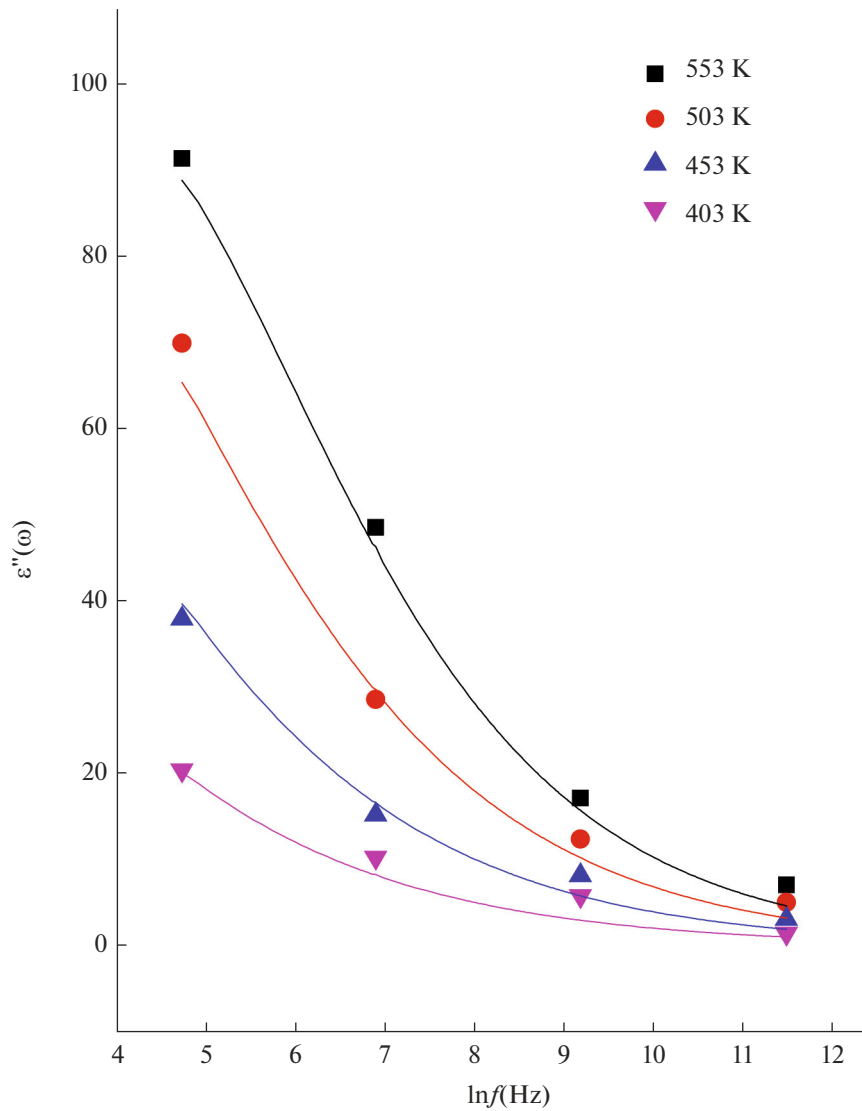


Fig. 11. Frequency dependence of the dielectric loss, solid curves represents the fitting according to Cole–Cole equation.

and

$$\varepsilon''(\omega) = \frac{(\varepsilon_0 - \varepsilon_\infty)[(\omega\tau_d)^{(1-\alpha)} \cos(\alpha\pi/2)]}{[1 + 2(\omega\tau_d)^{(1-\alpha)} \sin(\alpha\pi/2) + (\omega\tau_d)^{2(1-\alpha)}]}, \quad (14)$$

where ε_0 and ε_∞ are the lowest and highest frequency dielectric constants, τ_d is the dielectric relaxation time, α is an empirical factor having values $0 \leq \alpha \leq 1$. A magnitude of $\alpha = 0$ belongs to the Debye type relaxation [49]. The investigated $\varepsilon'(\omega)$ and $\varepsilon''(\omega)$ data are fitted effectively to the Eqs. (13) and (14). The value of α is fluctuated to get the best fits. M. Sayer and A. Mansingh [50] stated that the low magnitudes of $\alpha > 0.3$ reflects a limited dispersion of relaxation times. The obtained α values for the current glasses show a variety in the range between 0.13 and 0.55, which implies that these glasses display an enormous range of relaxation

times. Comparable values of $\alpha \approx 0.42\text{--}0.58$ are recorded for the $B_2O_3 \cdot CdSO_4$ glasses [10].

SUMMARY

A set of glasses of the composition $(100 - x)B_2O_3 \cdot xPbSO_4$ [$0 \leq x \leq 40$] are prepared by the press-quenching method for the glass melts. XRD analysis proved the complete amorphous nature of the glasses with no evidence for the presence of any crystallite peaks. Bulk density and O-ion density are found to increase with increasing the mol % $PbSO_4$ in the glasses, while the V_m values showed some variation with increasing the mol % $PbSO_4$. $[SO_4]^{2-}$ groups are proved to replace the BO_3 groups in the glass matrix, this in enables the jumping electrons/polarons become able to move easily between Pb and B ions. The dc and ac conductivi-

ties are investigated in the temperature range 303–673 K. The dc conduction mechanism is found to follow the Arrhenius equation with activation energies between 0.44 and 0.76 eV. The ac conductivity for all the glasses was found to increase from 1.1×10^{-7} to 1.2×10^{-4} S cm⁻¹ in the measuring frequency range. The moisture was found to greatly affect the ac conductivity results in the low temperature region because of the vibration of OH molecules. The ac conductivity shows good fittings to the PPT model as well as to the CBH model. All the calculated values for N , τ_0 and W_m are found to increase with increasing the mol % PbSO₄ in the glasses. Finally, the dielectric constant and the dielectric loss are measured and discussed as a function of the temperature. The experimental $\epsilon'(\omega)$ and $\epsilon''(\omega)$ data are fitted to the Cole–Cole relations with a large distribution of relaxation times ($\alpha \approx 0.13$ – 0.55).

FUNDING

Taif University Researchers Supporting Project number (TURSP2020/22), Taif University, Taif, Saudi Arabia.

CONFLICT OF INTEREST

The authors declare that they have no conflicts of interest.

DATA AVAILABILITY

The authors confirm that the data supporting the findings of this study are available within the article. Raw data that support the findings of this study are available from the corresponding author, upon reasonable request.

REFERENCES

- Krogh-Moe, J., The structure of vitreous and liquid boron oxide, *J. Non-Cryst. Solids*, 1969, vol. 1, p. 269.
- Frischat, G.H. and Szurman, M., Role of sulfur and its diffusion in silicate glass melts, *Int. J. Appl. Glass. Sci.*, 2011, vol. 2, p. 47.
- Rani, S., Sanghi, S., Anshu, Agarwal, A., Kishore, N., and Seth, V.P., Effect of ZnO/CdO on the structure and electrical conductivity in Li₂O–MO–Bi₂O₃–B₂O₃ glasses (M= Zn, Cd), *J. Phys. Chem. Solids*, 2008, vol. 69, p. 1855.
- Baia, L., Stefan, R., Kiefer, W., Popp, J., and Simon, S., Structural investigations of copper doped B₂O₃–Bi₂O₃ glasses with high bismuth oxide content, *J. Non-Cryst. Solids*, 2002, vol. 303, p. 379.
- Mozzi, R.L. and Warren, B.E., The structure of vitreous boron oxide, *J. Appl. Crystallogr.*, 1970, vol. 3, p. 251.
- Ahmed, E.M. and Gaml, E.A., Effect of Pb/B ion replacement in B₂O₃–PbO–Fe₂O₃–Na₂O glasses: Optical, magnetic, and fluorescence properties, *Opt. Mater.*, 2021, vol. 116, 111075.
- Abdel-Wahab, F., Mostafa, A.G., Belal, A.E., and El-Agwany, E.M., Mössbauer spectroscopy and electrical transport properties of iron doped sodium lead borate glasses, *J. Mater. Chem. Phys.*, 2005, vol. 93, no. 1, pp. 243–250.
- Dwivedi, B.P., Rahman, M.H., Kumar, Y., and Khanna, B.N., Raman scattering study of lithium borate glasses, *J. Phys. Chem. Solids*, 1993, vol. 54, no. 5, p. 621.
- Ahmed, E.M., Electric and dielectric properties of Cd-SO₄-doped borate glasses, *Int. J. Mod. Phys. B*, 2019, vol. 33, p. 1950011.
- El-Batal, F.H., Fayad, A.M., El-Rahman, S.A., and Moustafa, F.A., Effect of divalent metal oxides on absorption spectra of some sodium borate glasses containing mixed nickel and iron oxides, *Indian J. Pure Appl. Phys.*, 2006, vol. 44, p. 367.
- Bengisu, M., Borate glasses for scientific and industrial applications: A review, *J. Mater. Sci.*, 2016, vol. 51, no. 5, p. 2199.
- Mariselvam, K. and Kumar, R.A., Borate glasses for scientific and industrial applications: A review, *Univ. J. Chem.*, 2016, vol. 4, no. 2, p. 55.
- Segawa, H. and Hirosaki, N., Optical properties of zinc borate glasses dispersed with Eu-doped SiAlON for white LED applications, *Ceram. Int.*, 2018, vol. 44, p. 4783.
- Marion, N.W., Liang, W., Reilly, G., Day, D.E., Rahman, M.N., and Ma, J.J., Borate glass supports the in vitro osteogenic differentiation of human mesenchymal stem cells, *Mech. Adv. Mater. Struct.*, 2005, vol. 12, p. 1.
- Day, D.E., White, J.E., Brown, R.F., and McMenamin, K.D., Transformation of borate glasses into biologically useful materials, *Glass Technol.*, 2003, vol. 44, p. 75.
- Shimakawa, K., Kondo, A., Goto, M., and Long, A.R., AC loss originating from mesoscopic and macroscopic inhomogeneities in hydrogenated amorphous silicon, *J. Non-Cryst. Solids*, 1996, vol. 198, p. 157.
- Ghosh, A. and Chakravorty, D., Electrical conductivity in semiconducting CuO–Bi₂O₃–P₂O₅ glasses, *J. Phys: Condens. Matter*, 1990, vol. 2, p. 931.
- Datta, A., Giri, A.K., and Chakravorty, D., Ac electrical properties of sol-gel-derived glasses in the Sb₂O₃–SiO₂ system, *J. Phys: Condens. Matter*, 1992, vol. 4, p. 1783.
- Hazra, S. and Ghosh, A., AC electrical properties of sol-gel-derived glasses in the Sb₂O₃–SiO₂ system, *J. Phys: Condens. Matter*, 1997, vol. 9, p. 3981.
- Singh, R. and Chakravarthy, J.S., DC conductivity of V₂O₅-containing zinc tellurite glasses, *Phys. Rev. B*, 1997, vol. 55, p. 5550.
- Brahma, P., Banerjee, S., Chakraborty, S., and Chakravorty, D., Small polaron and bipolaron transport in antimony oxide doped barium hexaferrites, *J. Appl. Phys.*, 2000, vol. 88, p. 6526.
- Dyre, J.C. and Schroder, T.B., Universality of AC conduction in disordered solids, *Rev. Mod. Phys.*, 2000, vol. 72, no. 3, p. 873.
- Ahmed, E.M., El-Ghamaz, N.A., and Edres, A.M., Electrical conduction and switching properties of As₂O₃–V₂O₅–FeO glasses, *J. Mater. Sci.: Mater. Electron.*, 2018, vol. 29, no. 17, pp. 15191–15202.

24. Stroud, D., The effective medium approximations: Some recent developments, *Superlatt. Microstruct.*, 1998, vol. 23, nos. 3–4, p. 567.
25. Dyre, J.C., The random free-energy barrier model for AC conduction in disordered solids, *J. Appl. Phys.*, 1988, vol. 64, p. 2456.
26. Austin, I.G. and Mott, N.F., Polarons in crystalline and non-crystalline materials, *Adv. Phys.*, 1969, vol. 18, p. 41.
27. Elliott, S.R., AC conduction in amorphous chalcogenide and pnictide semiconductors, *Adv. Phys.*, 1987, vol. 36, p. 135.
28. Abdel-Wahab, F., Unified hopping model for DC and AC conduction in chalcogenide glasses, *Philos. Mag., B*, 2002, vol. 82, p. 1327.
29. Ahmed, E.M. and Abdel-Wahab, F., Unified conduction mechanism in unconventional VZnCaFeO glasses, *Phys. B (Amsterdam, Neth.)*, 2014, vol. 449, p. 246.
30. Alemi, A.A., Sedghi, H., Mirmohseni, A.R., and Golsanamlu, V., Synthesis and characterization of cadmium doped lead-borate glasses, *Bull. Mater. Sci.*, 2006, vol. 29, no. 1, pp. 55–58.
31. Ahmed, E.M., Elghamaz, N.A., and Edres, A.M., Thermal kinetics and theoretical third order nonlinear optical susceptibility of some $As_2O_3-V_2O_5-FeO$ glasses, *Phys. Stat. Solidi A*, 2018, vol. 215, p. 1800299.
32. Mori, H., Matsuno, H., and Sakata, H., Small polaron hopping conduction in $V_2O_5-Sb-TeO_2$ glasses, *J. Non-Cryst Solids*, 2000, vol. 276, pp. 78–94.
33. Kishore, S.N., Agarwal, A., Seth, V.P., and Sheoran, M.S., Thermal and electrical properties of $MoO_3-Bi_2O_3-B_2O_3$ glasses, *Indian J. Pure Appl. Phys.*, 2008, vol. 46, no. 10, p. 719.
34. Ahmed, E.M., Youssif, M.I., and Elzelaky, A.A., Electrical conductivity and breakdown properties of some erbium oxide doped phosphovanadate glasses, *J. Mater. Sci.: Mater. Electron.*, 2020, vol. 31, no. 15, p. 12216.
35. Ahmed, E.M., El-Ghamaz, N.A., and Albhbah, S.M., Limited frequency domain of the AC conductivity of some $As_2O_3-V_2O_5-CuO-Nd_2O_3$ glasses, *J. Non-Cryst. Solids*, 2021, vol. 558, 120659.
36. Rada, S., Rus, L., Rada, M., Culea, E., Aldea, N., Stan, S., Suci, R.C., and Bot, A., Synthesis, structure, optical and electrochemical properties of the lead sulfate-lead dioxide-lead glasses and vitroceraamics, *Solid State Ionics*, 2015, vol. 274, p. 111.
37. Pichavant, M., An experimental study of the effect of boron on a water saturated haplogranite at 1 kbar vapor pressure, *Contrib. Mineral. Petrol.*, 1981, vol. 76, p. 430.
38. Holtz, F., Behrens, H., and Dingwell, D.B., Effects of F, B_2O_3 and P_2O_5 on the solubility of water in haplogranite melts compared to natural silicate melts, *Contrib. Mineral. Petrol.*, 1993, vol. 113, p. 492.
39. Romano, C., Dingwell, D.B., and Hess, K.U., The effect of boron on the speciation of water in haplogranitic melts, *Period. Mineral.*, 1995, vol. 64, p. 413.
40. Schmidt, B.C. and Zotov, N., Ray dupree, structural implications of water and boron dissolution in albite glass, *J. Non-Cryst. Solids*, 2004, vol. 337, p. 207.
41. Dillip, K., Choudhary, R.N.P., and Samantaray, B.K., Studies of dielectric relaxation and AC conductivity behavior of plasticized polymer nanocomposite electrolytes, *Int. J. Electrochem. Sci.*, 2008, vol. 3, p. 597.
42. Alemi, A.A., Sedghi, H., Mirmohseni, A.R., and Golsanamlu, V., Synthesis and characterization of cadmium doped lead-borate glasses, *Bull. Mater. Sci.*, 2006, vol. 29, no. 1, p. 55.
43. Dyre, J.C., Universal low-temperature AC conductivity of macroscopically disordered nonmetals, *Phys. Rev. B*, 1993, vol. 48, p. 12511.
44. Abdel Wahab, F. and Ahmed, E.M., Correlation between microscopic and macroscopic conductivity models through Meyer-Neldel rule. I, *Rep. Phys.*, 2013, vol. 7, no. 1, pp. 44–48.
45. Long, A.R., Frequency-dependent loss in amorphous semiconductors, *Adv. Phys.*, 1982, vol. 31, p. 553.
46. Hazra, S. and Ghosh, A., Electrical relaxation mechanism in unconventional bismuth cuprate glasses, *J. Appl. Phys.*, 1998, vol. 84, p. 987.
47. Abdel-Wahab, F., Aziz, M.S., Mostafa, A.G., and Ahmed, E.M., Electrical conductivity and dielectric properties of some vanadium-strontium-iron unconventional oxide glasses, *Mater. Sci. Eng., B*, 2006, vol. 134, p. 1.
48. Cole, K.S. and Cole, R.S., Dispersion and absorption in dielectrics I. Alternating current characteristics, *J. Chem. Phys.*, 1941, vol. 9, p. 341.
49. Qiu, H.H., Ito, T., and Sakata, H., DC conductivity of $Fe_2O_3-Bi_2O_3-B_2O_3$ glasses, *Mater. Chem. Phys.*, 1998, vol. 58, p. 243.
50. Sayer, M. and Mansingh, A., Dielectric relaxation in vitreous GeO_2 , *Phys. Chem. Glasses*, 1982, vol. 23, p. 83.